


RESEARCH PAPER



An inverse interaction between *HOXA11* and *HOXA11-AS* is associated with cisplatin resistance in lung adenocarcinoma

Youwei Zhang^a, Yuan Yuan^a, Yang Li^b, Peiyong Zhang^a, Pingsheng Chen^c, and Sanyuan Sun ^a

^aDepartment of Medical Oncology, Affiliated Xuzhou Central Hospital, Southeast University, Xuzhou, China; ^bDepartment of Molecular Laboratory, Affiliated Xuzhou Central Hospital, Southeast University, Xuzhou, China; ^cDepartment of Pathology, School of Basic Medical Sciences, Southeast University, Nanjing, China

ABSTRACT

HOXA11, which is a member of the homeobox (*HOX*) gene family, and its natural antisense transcript (NAT) *HOXA11-AS* have been reported to be closely related to the development of lung cancer. We aimed to investigate their specific roles in cisplatin (DDP) resistance in lung adenocarcinoma (LUAD). First, we found that *HOXA11* is hypermethylated and significantly downregulated in a DDP-resistant A549 cell line (A549/DDP) and LUAD tissues, while the *HOXA11-AS* expression level is elevated. Although *HOXA11* and *HOXA11-AS* mRNA overlap in the 5'-untranslated region (5' UTR) and share two CpG islands, DNA methylation only regulates the expression of *HOXA11*. Then, we found that *HOXA11* and *HOXA11-AS* have an inverse interaction by transfecting their siRNAs and overexpression vectors into A549 and A549/DDP cells. A dual-luciferase reporter assay further confirmed that the overlapping 5'UTR is essential for the bidirectional regulation between *HOXA11* and *HOXA11-AS*. Functional analysis showed that knockdown of *HOXA11* expression in A549 cells induced DDP resistance and activated *Akt/β-catenin* signaling, while overexpression of *HOXA11* in A549/DDP cells increased DDP sensitivity and inhibited *Akt/β-catenin* signaling. Moreover, *HOXA11-AS* knockdown in A549 cells increased DDP sensitivity and inhibited *Akt/β-catenin* signaling, while the overexpression of *HOXA11-AS* in A549/DDP cells induced DDP resistance and activated *Akt/β-catenin* signaling. In conclusion, our study demonstrates that the inverse interaction between *HOXA11* and *HOXA11-AS* promotes DDP resistance in LUAD.

ARTICLE HISTORY

Received 25 February 2019
Revised 21 May 2019
Accepted 23 May 2019

KEYWORDS

Lung adenocarcinoma;
resistance; methylation;
HOXA11; *HOXA11-AS*

Introduction

Lung cancer leads to the most cancer-related deaths worldwide, and non-small cell lung cancer (NSCLC) accounts for approximately 80% of all lung cancer cases [1]. Lung adenocarcinoma (LUAD) has been the fastest growing subtype of NSCLC in recent years. Platinum-based doublets are widely used as a first-line NSCLC treatment and improve survival rates compared to placebo treatments [2]. Although many innovative drugs, including epidermal growth factor receptor (EGFR)-tyrosine kinase inhibitors (TKIs) and checkpoint inhibitors, have made substantial progress in the treatment of LUAD, chemotherapy remains the standard treatment, and the combination of chemotherapy and molecular targeted therapy or immunotherapy has become a new therapeutic strategy [3,4]. Cisplatin (DDP), which disrupts the structure and function of DNA, is the most commonly used platinum agent for lung cancer [5]. However,

resistance to DDP eventually develops and then induces recurrence, invasion and therapeutic failure [6]. Several cellular events involved in chemoresistance have been revealed, such as DNA methylation, noncoding RNA, stem cells and autophagy [7–9], but these events are not yet clearly defined. Therefore, an improved understanding of the molecular mechanism of DDP resistance is required for the advancement of LUAD treatment.

Our previous studies have demonstrated a panel of candidate genes that are downregulated by DNA methylation-induced DDP resistance in NSCLC using high-throughput microarrays [10,11]. We also found that *HOXA11*, a member of the homeobox (*HOX*) gene family, is hypermethylated and significantly downregulated in the resistant A549/DDP cell line, while in the parental A549 cells, *HOXA11* is hypomethylated and overexpressed. Many other studies have confirmed that *HOXA11*

expression is downregulated in human gastric cancer [12], renal cell carcinoma [13], glioblastoma [14] and LUAD [15]. Furthermore, hypermethylation may cause *HOXA11* inactivation and contribute to the progression of NSCLC by promoting cell proliferation or migration, suggesting the tumor-suppressive function of *HOXA11* [16].

Interestingly, *HOXA11-AS*, which is the natural antisense transcript (NAT) of *HOXA11*, has been reported to be upregulated in various types of carcinomas and is generally associated with increased lymph node metastasis, advanced tumor stage, poor tumor differentiation, and poor prognosis [17,18]. *In vitro* and *in vivo* assays have revealed that *HOXA11-AS* acts as an oncogenic long noncoding RNA (lncRNA) that promotes cell growth and metastasis by recruiting multiple chromosome-modifying enzymes to target genes or by sponging specific microRNAs (miRNA) [19,20]. A latest study also found that *HOXA11-AS* promotes cisplatin resistance in human LUAD cells by modulating miR-454-3p/Stat3 [21].

Because *HOXA11* and *HOXA11-AS* have a complementary overlap in the 5'-untranslated region (5' UTR) in a head-to-head (5'-5') manner and share two CpG islands that are sites of hypermethylation, we aimed to determine the interactions between *HOXA11* and *HOXA11-AS*. Thus, in the present study, we explored the roles of *HOXA11* and *HOXA11-AS* in DDP resistance in LUAD.

Results

The expression status of HOXA11 and HOXA11-AS in DDP-resistant LUAD cell lines and tissues

Information from the National Center for Biotechnology Information gene database (<http://www.ncbi.nlm.nih.gov/gene>) shows that *HOXA11* and *HOXA11-AS* mRNA overlap at the 5'UTR in a head-to-head manner (Figure 1) and that *HOXA11* and *HOXA11-AS* mRNA share two CpG islands (CpG 1, chr7:27225050–27225629; CpG 2, chr7:27224267–27224596).

Real-time PCR was used to analyze the expression of *HOXA11* and *HOXA11-AS*, and qMSP and BSP were used to evaluate their methylation status. The results showed that *HOXA11-AS* expression was upregulated and that *HOXA11* expression was downregulated in the DDP-resistant A549/DDP cell line, with hypermethylation of CpG 1 and CpG 2 compared to the parental A549 cell line. After 5-aza-2'-deoxycytidine (5-aza-CdR) treatment (1 μ M), *HOXA11* expression was restored in A549/DDP cells, and the methylation statuses of CpG 1 and CpG 2 were reversed, while the expression of *HOXA11-AS* was not affected (Figure 2(a-c)). Thus, *HOXA11* expression is mainly regulated by DNA methylation, whereas its antisense RNA *HOXA11-AS* is regulated by other mechanisms.

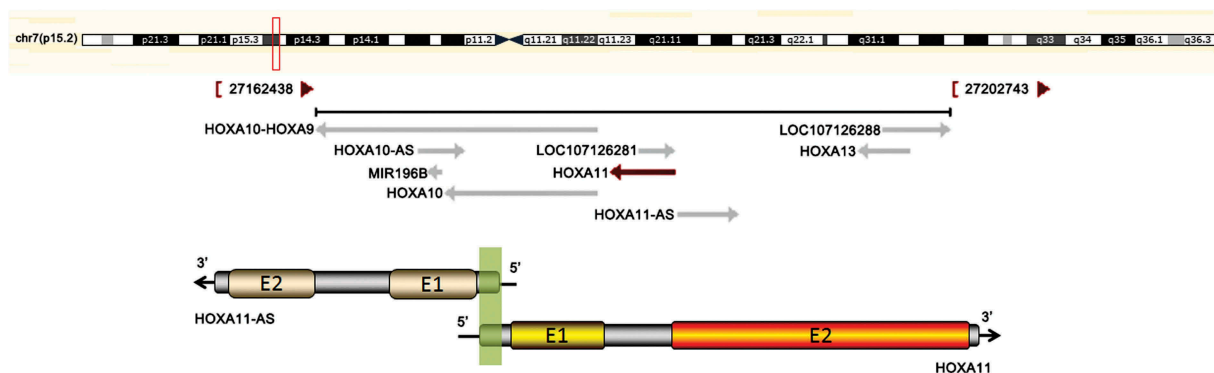


Figure 1. The correlation between *HOXA11* and *HOXA11-AS* mRNA. The upper chart in this panel shows the genomic locus of *HOXA11* indicated on the UCSC site. The lower chart in this panel is a schematic of *HOXA11-AS* and *HOXA11* mRNA. 'E' indicates exons. The green shadow indicates the overlapping region of *HOXA11-AS* and *HOXA11* mRNA. The black arrows show the direction of transcription.

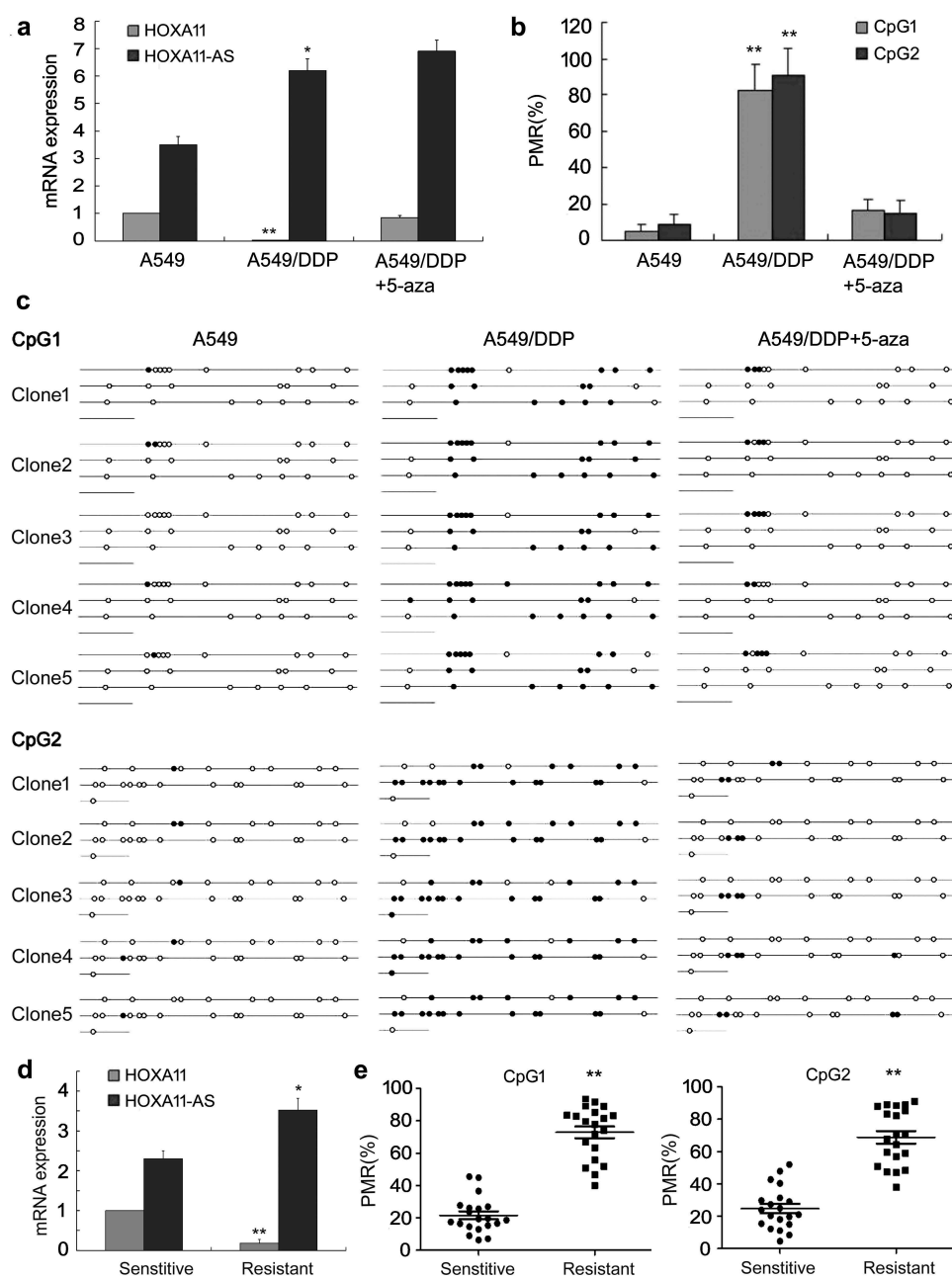


Figure 2. The expression status of *HOXA11-AS* and *HOXA11* in cisplatin (DDP)-resistant lung adenocarcinoma cell lines and tissues. Real-time PCR (a) was used to analyze the expression of *HOXA11-AS* and *HOXA11*. qMSP (b) and BSP (c) were used to evaluate their methylation statuses. *HOXA11-AS* expression was upregulated and *HOXA11* expression was downregulated in the A549/DDP cell line, with hypermethylation of CpG 1 and CpG 2. Treatment with 5-aza-CdR (1 μ M) restored *HOXA11* expression and reversed the hypermethylation of the CpG islands. The *HOXA11-AS* and *HOXA11* expression status (d) and methylation (e) were also analyzed in primary tumor cells; 20 LUAD samples were considered DDP-sensitive samples ($IC_{50} < 5$ mg/L), and 20 samples were considered DDP-resistant samples ($IC_{50} > 10$ mg/L). PMR, percentage of methylation reference.

Using primary tumor cell culture and drug susceptibility testing, 20 LUAD samples were considered DDP-sensitive samples ($IC_{50} < 5$ μ g/mL), and 20 samples were considered DDP-resistant samples

($IC_{50} > 10$ μ g/mL). The results showed that the expression of *HOXA11-AS* was upregulated and that the expression of *HOXA11* was downregulated in the DDP-resistant tissues (Figure 2(d)), with

a higher percentage of methylation reference (PMR) of CpG 1 and CpG 2 (Figure 2(e)) compared to sensitive tissues.

The inverse interaction between *HOXA11* and *HOXA11-AS* through the overlapping 5'UTR

The common function of antisense transcripts is the regulation of the expression of sense transcripts. To investigate the relationship between *HOXA11* and *HOXA11-AS*, specific siRNAs that target their non-overlapping regions were transfected into the A549 cell line, and *HOXA11* and *HOXA11-AS* overexpression vectors were transfected into A549/DDP cells. The results showed that the knockdown of *HOXA11* and *HOXA11-AS* mRNA expression by siRNA increased the expression levels of their respective counterparts in A549 cells, while the overexpression of *HOXA11* and *HOXA11-AS* mRNA led to a significant decrease in the expression levels of their respective counterparts in A549/DDP cells (Figure 3(a,b)). siRNA targeting *HOXA11-AS* also increased the protein expression level of *HOXA11* in A549 cells, and the overexpression of *HOXA11-AS* reduced the protein expression level of *HOXA11* in A549/DDP cells (Figure 3(c)). Furthermore, the mRNA expression levels of *HOXA11* and *HOXA11-AS* were negatively correlated in primary cultured tumor cells, regardless of DDP sensitivity or resistance (Figure 3(d)). Finally, we performed a dual-luciferase reporter assay to investigate the role of the overlapping 5'UTR, and the result showed that *HOXA11-AS* overexpression decreased the 5'UTR luciferase activity of *HOXA11* in A549 cells, while the mutant overlapping sequence abrogated this effect (Figure 3(e)). Thus, the overlapping 5'UTR is essential for the bidirectional regulation between *HOXA11* and *HOXA11-AS*.

***HOXA11* and *HOXA11-AS* function in DDP resistance in vitro**

To investigate the function of *HOXA11* and *HOXA11-AS* in DDP resistance, their specific siRNAs were transfected or cotransfected into A549 cells, and their overexpression vectors were transfected or cotransfected into A549/DDP cells. Then, a CCK-8 assay, flow cytometry and TUNEL assay were performed. The knockdown of *HOXA11* expression

caused cell proliferation to increase significantly (Figure 4(a)), and the IC₅₀ values of DDP increased in A549 cells (Figure 4(b)). Additionally, the G₁ phase of the cell cycle was decreased and the S phase was increased, but cell apoptosis did not decrease significantly (Figure 4(c)). Conversely, the knockdown of *HOXA11-AS* expression caused cell proliferation to be significantly inhibited (Figure 4(a)), and the IC₅₀ values of DDP decreased (Figure 4(b)) in A549 cells; besides, the G₁ phase of the cell cycle and cell apoptosis were significantly increased (Figure 4(c)). When the specific siRNAs of *HOXA11* and *HOXA11-AS* were cotransfected into A549 cells, their respective effects on cell proliferation, cell cycle and apoptosis were weakened (Figure 4(a-c)), indicating that *HOXA11* and *HOXA11-AS* biologically antagonize each other.

Similarly, the overexpression of *HOXA11* in A549/DDP cells resulted in a significant inhibition of cell proliferation (Figure 4(a)), decrease of the IC₅₀ values of DDP (Figure 4(b)), and increase of cell cycle G₁ phase and cell apoptosis (Figure 4(d)). However, the overexpression of *HOXA11-AS* caused cell proliferation and the IC₅₀ values of DDP to increase significantly in A549/DDP cells (Figure 4(a,b)). Additionally, the S phase of the cell cycle was increased, but cell apoptosis was not significantly affected (Figure 4(d)). When the overexpression vectors of *HOXA11* and *HOXA11-AS* were cotransfected into A549/DDP cells, their respective effects on cell proliferation, cell cycle and apoptosis were weakened (Figure 4(a,b,d)).

Furthermore, the knockdown of *HOXA11* expression in A549 cells caused the downregulation of *p21* (negative regulatory protein of cell cycle), *bax*, cleaved *caspase 3* (apoptotic protein), and *VEGF* (vascular endothelial growth factor) expression and the upregulation of *cyclin D1* (positive regulatory protein of cell cycle), *bcl-2* (antiapoptotic protein), *β-catenin* and *p-AKT* (activated signaling pathway) expression, while the knockdown of *HOXA11-AS* expression caused the opposite effects in A549 cells. The overexpression of *HOXA11* in A549/DDP cells caused the upregulation of *p21*, *bax*, cleaved *caspase 3*, and *VEGF* expression and the downregulation of *cyclin D1*, *bcl-2*, *β-catenin* and *p-AKT* expression, while the overexpression of *HOXA11-AS* caused the opposite effects in A549/DDP cells (Figure 5).

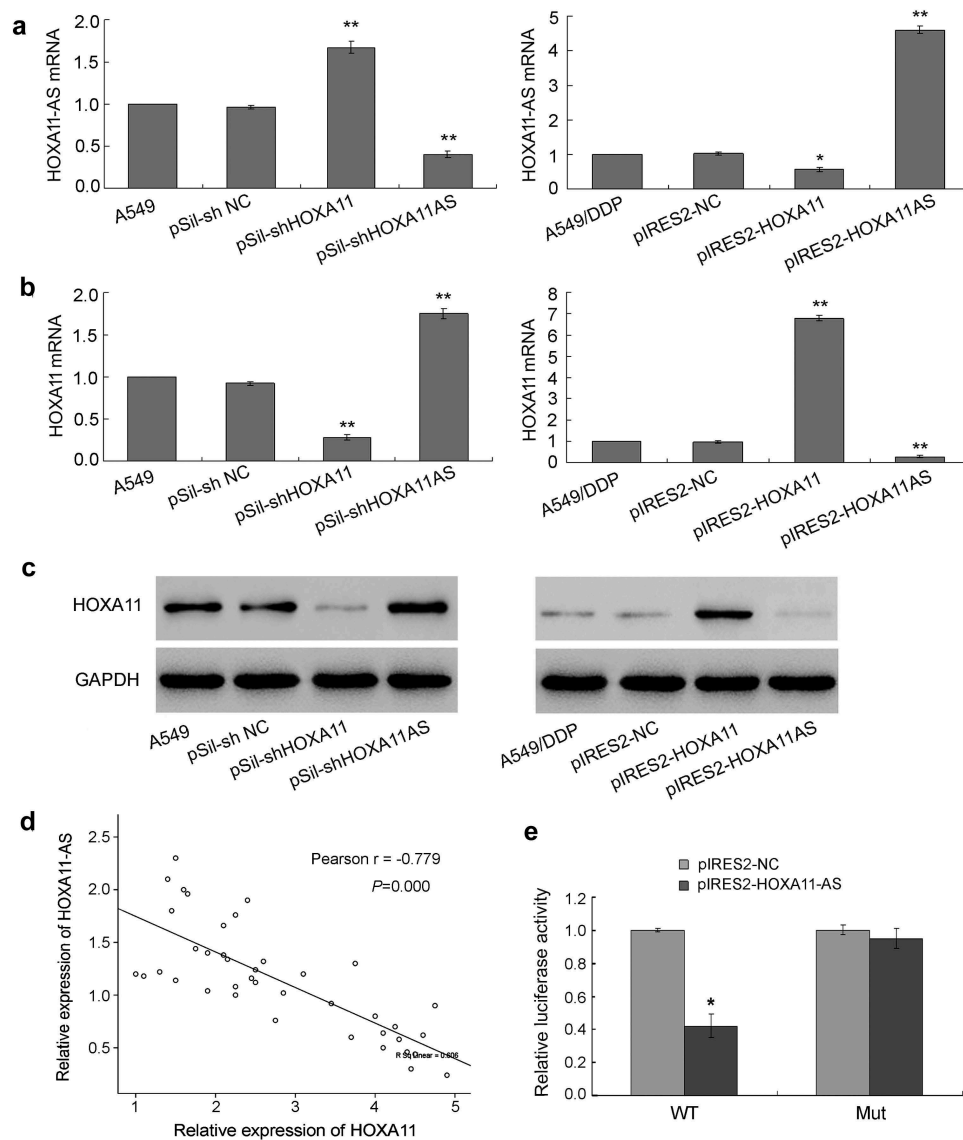


Figure 3. The inverse interaction between *HOXA11* and *HOXA11-AS*. (a) The effects of *HOXA11* and *HOXA11-AS* siRNA on the mRNA expression of *HOXA11-AS* in A549 cells. The effects of the *HOXA11* and *HOXA11-AS* overexpression vectors on the mRNA expression of *HOXA11-AS* in A549/DDP cells. (b) The effects of *HOXA11* and *HOXA11-AS* siRNA on the mRNA expression of *HOXA11* in A549 cells. The effects of the *HOXA11* and *HOXA11-AS* overexpression vectors on the mRNA expression of *HOXA11* in A549/DDP cells. (c) The effects of *HOXA11* or *HOXA11-AS* siRNA on the protein expression of *HOXA11* in A549 cells. The effects of the *HOXA11* and *HOXA11-AS* overexpression vectors on the protein expression of *HOXA11* in A549/DDP cells. (d) The mRNA expression levels of *HOXA11* and *HOXA11-AS* were negatively correlated in primary cultured tumor cells regardless of cisplatin sensitivity or resistance. (e) The luciferase activity in A549 cells cotransfected with luciferase reporters containing wild-type (WT) or mutant (mut) 5'UTR overlapping sequence and pIRES2-*HOXA11-AS* or negative control. The data are presented as the relative ratio of firefly luciferase activity to Renilla luciferase activity. * $P < 0.05$ vs. NC; ** $P < 0.01$ vs. NC.

***HOXA11* and *HOXA11-AS* function in DDP resistance in vivo**

Mice were separated into eight groups (five mice per group) according to the inoculated cells. In mice inoculated with A549 cells, the knockdown of *HOXA11* expression caused cell proliferation to

increase significantly, while the knockdown of *HOXA11-AS* expression inhibited cell proliferation, and A549 cells cotransfected with siRNAs of *HOXA11* and *HOXA11-AS* attenuated their respective effects (Figure 6(a,b)). In mice inoculated with A549/DDP cells, the overexpression of

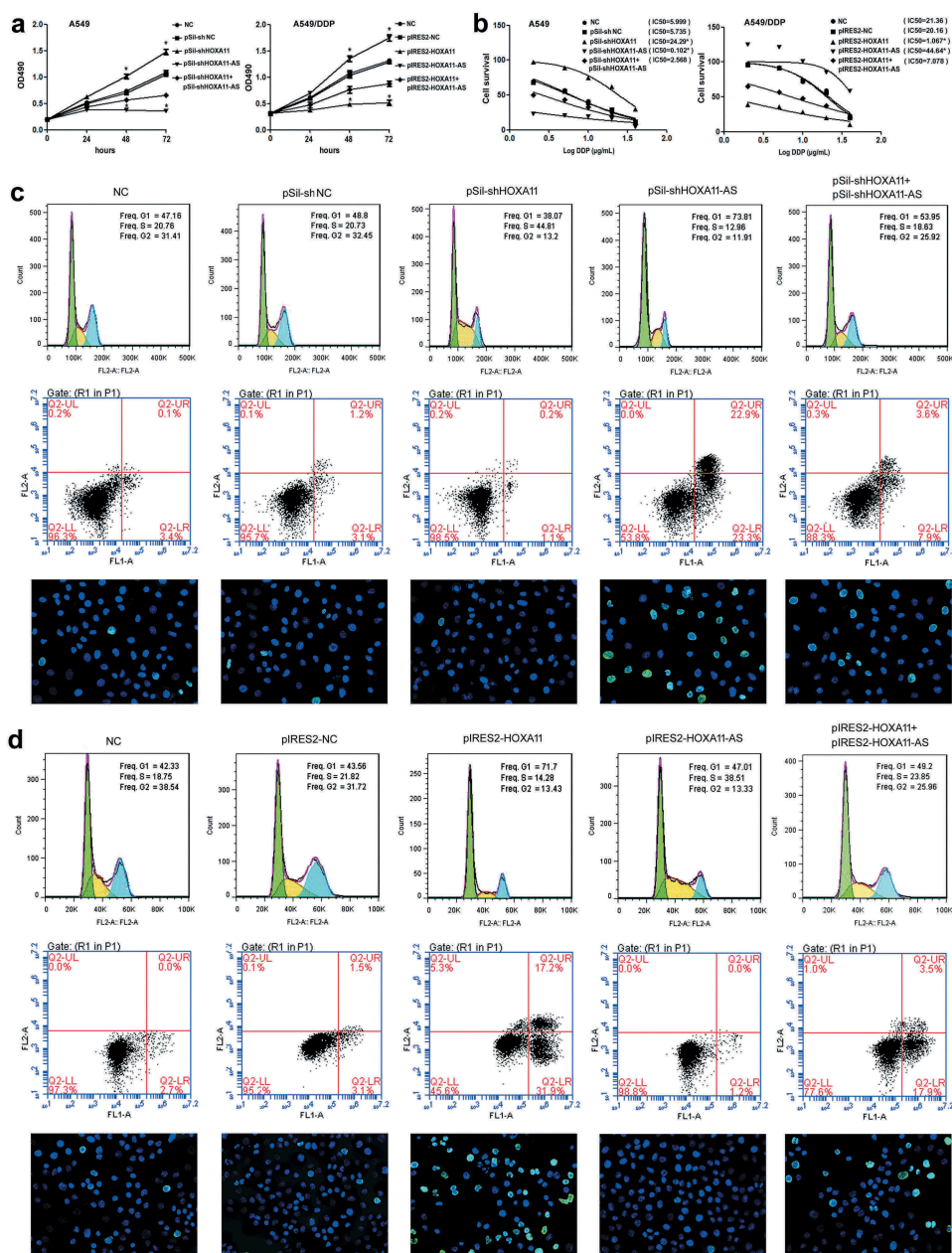


Figure 4. The functions of *HOXA11* and *HOXA11-AS* in cisplatin (DDP) resistance *in vitro*. *HOXA11*- and *HOXA11-AS*-specific siRNAs were transfected or cotransfected into A549 cells, and *HOXA11* and *HOXA11-AS* overexpression vectors were transfected or cotransfected into A549/DDP cells. Using a CCK-8 assay, cell proliferation was analyzed (a), and the IC₅₀ values of DDP were calculated (b). Flow cytometry and TUNEL assays revealed the cell cycle and apoptosis in A549 (c) and A549/DDP cells (d).

HOXA11 significantly inhibited cell proliferation, while the overexpression of *HOXA11-AS* increased cell proliferation, and A549/DDP cells cotransfected with vectors of *HOXA11* and *HOXA11-AS* attenuated their respective effects (Figure 6(a,c)). These results further indicated the tumor-suppressive role of the *HOXA11* gene and the oncogenic role of *HOXA11-AS* in DDP resistance of LUAD.

Discussion

In the present study, we first found that *HOXA11* is hypermethylated and significantly downregulated in the DDP-resistant A549 cell line and LUAD tissues and that the 5-aza-CdR treatment restores *HOXA11* expression and reverses the hypermethylation of CpG islands. *HOX* genes encode transcription factors that play crucial roles in a wide range of processes,

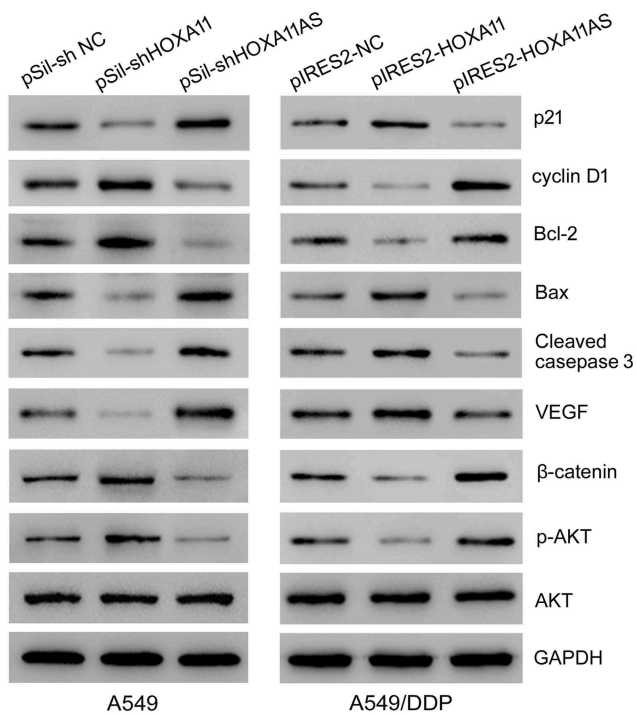


Figure 5. The effects of *HOXA11* and *HOXA11-AS* on cellular function-related proteins. Western blot analysis of the protein expression levels in A549 cells with *HOXA11* or *HOXA11-AS* knockdown and the protein expression levels in A549/DDP cells with *HOXA11* or *HOXA11-AS* overexpression.

including apoptosis, differentiation, motility, and angiogenesis. In humans, *HOX* genes are arranged into four clusters (A, B, C, and D) on different

chromosomes, and 39 *HOX* genes have been identified [22]. *HOX* genes are also known to play an essential role in lung development and are expressed in the normal human adult lungs [23]. The *HOXA* cluster, which is located on chromosome 7p15–7p14.2, consists of 12 genes, including *HOXA11* [24]. Highly dense CpG islands are prevalent in most *HOXA* promoters, and *HOXA11* hypermethylation has recently been reported in breast [25], gastric [12,26], ovarian [27] and cervical cancers [28] and in renal cell carcinoma [13]. The methylation of *HOXA11* has also been proposed as an early detection marker and as a poor prognostic marker in certain types of cancers [25,27,28], and functional studies have shown that *HOXA11* acts as a tumor suppressor gene [12,13]. In lung cancer, *HOXA11* has been verified as one of the most frequently hypermethylated genes using high-throughput DNA methylation arrays [29,30]. Furthermore, Hwang et al [6]. revealed that *HOXA11* hypermethylation occurred in 218 (69%) of 317 primary NSCLC cases, 5-Aza-dC treatment restores the expression of *HOXA11* in lung cancer cell lines, and transient transfection of *HOXA11* into H23 cells results in the inhibition of cell proliferation and migration. Li et al [5]. also found aberrant hypermethylation, and the methylation-induced downregulation of *HOXA11* might be a diagnostic and prognostic marker in patients with LUAD.

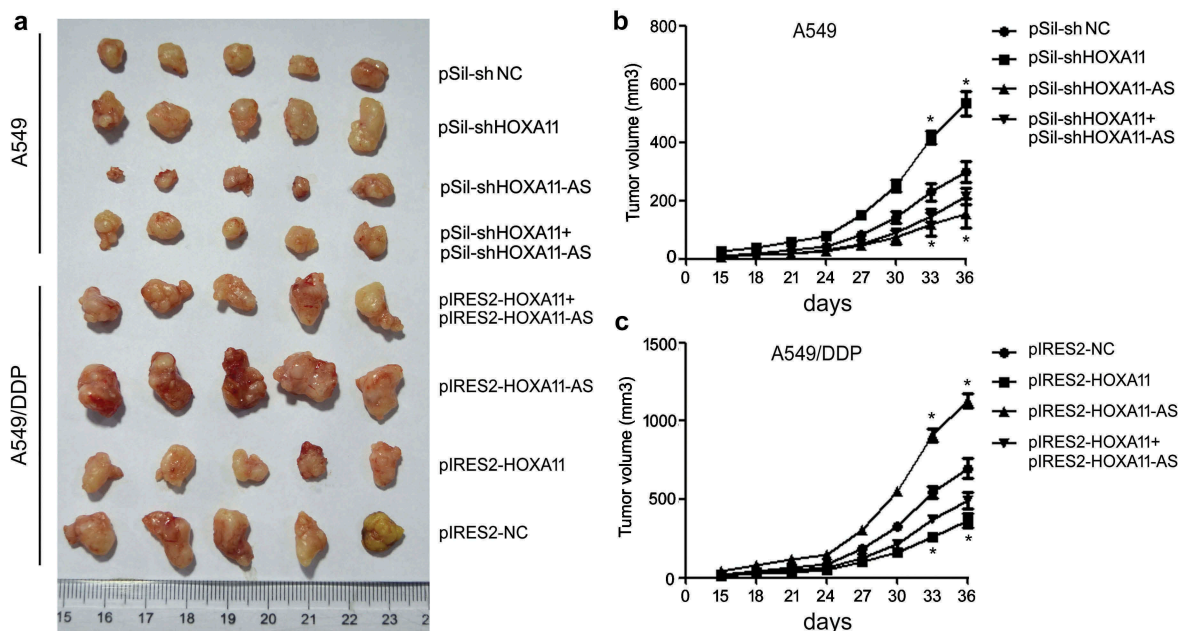


Figure 6. The functions of *HOXA11* and *HOXA11-AS* in cisplatin (DDP) resistance *in vivo*. Cells (2×10^6 cells/100 μ l PBS) were subcutaneously inoculated into the right flank of BALB/c nu/nu mice, and the animals were randomly separated into eight groups (five per group) according to the inoculated cells. The mice were sacrificed, and the tumors were isolated after 36 days (a). The tumor size was monitored every 3 days after A549 (b) or A549/DDP (c) cell implantation.

However, a meta-analysis of data gathered from The Cancer Genome Atlas (TCGA) and Oncomine microarrays of 934 LUAD and 319 normal control tissues (the normal controls included tissues from healthy individuals combined with adjacent tumor samples and only 32 pairs of LUAD tissues and adjacent nontumorous tissues) revealed that *HOXA11* is significantly overexpressed in LUAD tissues and that the expression level of *HOXA11* is significantly higher in patients with lymphoid metastases and an advanced clinical stage, indicating the potential oncogenic role of *HOXA11* in the genesis of LUAD [31]. Similar results have also been reported in lung squamous cell carcinoma (LUSC) by bioinformatics analysis [32]. Thus, the molecular mechanisms of *HOXA11* in lung cancer pathogenesis mostly remain elusive and require further investigation.

Investigations of *HOXA11* in DDP-resistant lung cancer are even more deficient. Se et al [1], have indicated that a reduction in the expression level *HOXA11* induces decreased anticancer effects of radiotherapy and/or temozolomide and leads to a poor prognosis in glioblastoma. In a phase II clinical trial, the demethylation reagent decitabine was shown to alter the DNA methylation of *HOXA11*, restoring sensitivity to carboplatin in patients with platinum-resistant ovarian cancer [33]. Consistent with these results, our research confirmed that the knockdown of *HOXA11* expression in A549 cells increases cell proliferation, decreases the G₁ phase of the cell cycles, increases the S phase of the cell cycle, induces DDP resistance *in vitro* and *in vivo*. Western blot analysis showed activation of the *Akt* and β -*catenin* signaling proteins, accompanied by corresponding changes in the cell cycle and apoptosis-related proteins. Conversely, the overexpression of *HOXA11* in A549/DDP cells was shown to inhibit cell proliferation, induce G₁ phase cell cycle arrest and apoptosis, increase DDP sensitivity *in vitro* and *in vivo*, and inhibit the *Akt* and β -*catenin* signaling proteins, indicating that *HOXA11* acts as a tumor suppressor gene against DDP-resistant human LUAD cells likely by inhibiting the *Akt*/ β -*catenin* signaling pathway.

Furthermore, we found that *HOXA11-AS*, the NAT of *HOXA11*, was upregulated in the DDP-resistant A549 cell line and LUAD tissues. Functional analysis showed that the knockdown of *HOXA11-AS* expression in A549 cells inhibits cell proliferation, induces G₁ phase cell cycle arrest and

apoptosis, increases DDP sensitivity *in vitro* and *in vivo*, and inhibits the *Akt* and β -*catenin* signaling proteins and that the overexpression of *HOXA11-AS* in A549/DDP cells caused the opposite effects, indicating that *HOXA11-AS* acts as an oncogene to promote DDP resistance in human LUAD cells likely by activating the *Akt*/ β -*catenin* signaling pathway. Growing evidences have demonstrated that *HOXA11-AS* lncRNA plays key roles in the development and progression of cancers [34–36]. Recently, a total of eight eligible studies consisting of 1320 patients with cancer were subjected to a meta-analysis, and the results revealed that an increased expression level of *HOXA11-AS* is significantly associated with increased lymph node metastasis, advanced tumor stage, poor tumor differentiation, and shorter overall survival (OS) and progression-free survival (PFS) [18]. Bioinformatics analyses have further indicated that *HOXA11-AS* is significantly overexpressed in both LUAD and LUSC tissues based on the TCGA database and have predicted that *HOXA11-AS* functions by regulating various pathways and genes [37]. Moreover, the knockdown of *HOXA11-AS* expression inhibits the proliferation, migration, invasion, and tumorigenic and angiogenic abilities of NSCLC cell lines and induces apoptosis and cell cycle arrest at the G₀/G₁ or G₂/M phase [20]. Chen et al [8,38], also found that *HOXA11-AS* expression is significantly upregulated in NSCLC tissues compared with adjacent normal tissues and that higher *HOXA11-AS* expression levels are associated with a poor prognosis in patients with NSCLC. The mechanistic findings showed that *HOXA11-AS* recruits the histone methyltransferase enhancer of zeste homologue 2 (*EZH2*) and DNA methyltransferase 1 (*DNMT1*) to the miR-200b promoter regions to repress miR-200b expression in NSCLC cells, promoting the epithelial-mesenchymal transition (EMT) in NSCLC cells. A recent study demonstrated that *HOXA11-AS* acts as a competing endogenous RNA (ceRNA) to promote DDP resistance in human LUAD cells via the miR-454-3p/Stat3 axis through the knockdown of *HOXA11-AS* expression in DDP-resistant A549 and H157 cell lines [21]. These results are all consistent with the results from our present study.

NATs, which are also known as natural antisense RNA, are endogenous transcripts containing sequences that are complementary to their sense RNAs. They encode either mRNA or noncoding

RNA and are mainly divided into the following two types: cis-NATs and trans-NATs. Cis-NATs are further classified according to their relative orientation and degree of overlap as follow: head-to-head (5' to 5'), tail-to-tail (3' to 3') and fully overlapping [39]. Recently, NATs have been found to play important roles in the development of cancers by directly interacting with sense transcripts. For example, *KRT7-AS* promotes gastric cancer cell proliferation and migration by forming an RNA-RNA duplex to stabilize *KRT7* mRNA [40]. *ZEB1-AS1* acts as an oncogene in osteosarcoma by epigenetically activating *ZEB1* [41], while *FOXC2-AS1* promotes doxorubicin resistance in osteosarcoma by increasing the expression level of *FOXC2* [42].

HOXA11-AS and its sense RNA *HOXA11* overlap in the 5' UTR region in a head-to-head manner and share two CpG islands. However, in our study, the expression statuses of *HOXA11* and *HOXA11-AS* in LUAD cells were completely opposite, and their regulation mechanisms were different. *HOXA11* expression is mainly regulated by DNA methylation, whereas *HOXA11-AS* is not affected by methylation. Additionally, their biological functions in LUAD cells were antagonistic, and cotransfection of *HOXA11*- and *HOXA11-AS*-specific siRNAs into A549 cells or cotransfection of *HOXA11* and *HOXA11-AS* overexpression vectors into A549/DDP cells weaken their individual roles. The dual-luciferase reporter assay confirmed that *HOXA11* and *HOXA11-AS* were inversely and bidirectionally regulated via the overlapping 5'UTR. However, the specific interaction mechanisms between *HOXA11* and *HOXA11-AS* require further investigation.

Overall, our study demonstrates that the inverse interaction between *HOXA11* and *HOXA11-AS* promotes DDP resistance, providing new insight into the mechanisms underlying *HOXA11-AS* lncRNA through overlapping regions with sense transcripts and contributing to developments in

LUAD treatment because increasing the sensitivity to DDP has been considered as a potentially effective strategy to overcome cancer.

Materials and methods

Cell culture

The A549 human LUAD cell line was purchased from Shanghai Institutes for Biological Sciences, Chinese Academy of Cell Resource Center. The construction and culture of the DDP-resistant A549/DDP cell line were based on our previous study [8]. For treatment with 5-aza-CdR (Sigma Aldrich, St. Louis, MO), which is a specific DNA methyltransferase inhibitor, the cell culture medium was changed every 24 h. Primary LUAD cell isolation from fresh tumors, culture and identification of DDP sensitivity have been described previously [8].

Real-time quantitative PCR

Total RNA was isolated using TRIzol reagent (Thermo Fisher Scientific, Waltham, MA). First-strand cDNA was synthesized using 2 µg of total RNA with a reverse transcription kit (TaKaRa, Dalian, China). For amplification, cDNA was initially denatured at 95°C for 20 s, followed by 40 cycles at 95°C for 5 s, and annealing at 60°C for 30 s in an ABI 7300 thermocycler (Applied Biosystems, Foster City, CA) using Power SYBR Green (TaKaRa). The specific primer sequences for each gene are shown in Table 1. The relative expression levels of the genes were calculated by the $2^{-\Delta\Delta C_t}$ method.

Analysis of the methylation status

After genomic DNA extraction and spectrophotometric quantification, 1 µg of genomic DNA was treated with bisulfite using an EZ-DNA Methylation Gold Kit (Zymo Research, Orange, CA). Quantitative

Table 1. List of primers.

Gene	Forward(5'-3')	Reverse (5'-3')	Product (bp)
HOXA11	ggaaatgctcagaggcagtc	atcttcctgtgcccagttg	209
HOXA11-AS	tctcctggagtctcgatt	tcggaagtgaccatgaatga	197
CpG1 (MSP)	gggaagcgtttttgtttc	tcaaatcaccgtacaaatcg	106
CpG1 (USP)	tttgggaagtgtttttgtttt	tcaaatcaccatacaaatcaaac	106
CpG1 (BSP)	gtgtaattatgttggtgggg	aacaaaccacaaacaaacac	387
CpG2 (MSP)	gggtgtctaggtgtttc	cgacgtacctaacgacgtac	152
CpG2 (USP)	ggggtgttaggtgtttt	ccaacatacctaacaacatac	152
CpG2 (BSP)	gggtagttttaattattgggg	cctccttctaccaactacata	364

methylation-specific PCR (qMSP) was then performed in an ABI 7300 thermocycler using a SYBR Premix Ex Taq kit (TaKaRa). The specific primer sequences for each gene were designed by Methyl Primer Express® Software v1.0 and are shown in Table 1. *β-actin* (ACTB) was used to normalize the expression levels of the input DNA. The amount of methylated DNA was determined by the threshold cycle number (Ct) of each sample and presented as the percentage of methylation reference (PMR). For bisulfite sequencing (BSP), the bisulfite-treated DNA was amplified by PCR with BSP primers, and the PCR products were cloned into a pUC57 vector (GenScript, Nanjing, China). Five clones were selected and sequenced for each sample.

Transient transfection

The gene-expressing plasmids (pIRES2-*HOXA11* and pIRES2-*HOXA11AS*) and gene-interfering plasmids (pSIL-*HOXA11* and pSIL-*HOXA11AS*) were all constructed by GenePharma Corp (Suzhou, China). pIRES2-EGFP and pSIL-eGFP control vectors were purchased from Addgene (Cambridge, MA, USA). These recombinant vectors were transfected into cells using Lipofectamine 3000 (Invitrogen, Carlsbad, CA) according to the manufacturer's instructions. After 48 h, the cells were collected for subsequent experiments.

Western blotting

Cell protein lysates were separated by 10% sodium salt (SDS)-Polyacrylamide gel electrophoresis (PAGE) and blotted onto a polyvinylidene fluoride (PVDF) membrane (Roche Diagnostics, Mannheim, Germany). After soaking the membrane in 10 mL of 5% nonfat milk in Tris-buffered saline with tween 20 (TBST) solution for 1 h, the membrane was incubated with primary antibodies specific to *HOXA11*, *p21*, *cyclin D1*, *bcl-2*, *bax*, cleaved *caspase 3*, *VEGF*, *β-catenin*, *p-AKT*, *AKT* and *GAPDH* (Univ-bio Inc., Shanghai, China). Horseradish peroxidase-conjugated goat anti-rabbit IgG was used as a secondary antibody. The results were observed following a treatment with an enhanced chemiluminescent (ECL) substrate (Merck Millipore, Hong Kong, China).

Dual-luciferase reporter assay

Luciferase reporter gene vectors were constructed with *HOXA11* mRNA 5'UTR sequences and mutant 5'UTR sequences in pGL3 plasmids (GenePharma). The *HOXA11-AS1* sequence was subcloned into a pcDNA3.1 vector (GenePharma), and an empty pcDNA3.1 vector was used as a control. A549 cells were cotransfected with the wild-type (or mutant-type) pGL3 plasmid and pcDNA3.1 plasmid containing the *HOXA11-AS1* sequence (or the control pcDNA3.1 plasmid) by using Lipofectamine 3000 (Invitrogen). Luciferase activity was measured with a Dual-Luciferase Reporter Assay System (Promega Corporation, Fitchburg, WI) after 48 h and presented as the ratio between firefly and Renilla luciferase activity (Fluc/Rluc).

Cell viability and proliferation analysis

Cell viability was assessed using a cell counting kit-8 (CCK-8) assay. Briefly, cells were seeded into 96-well plates at an initial density of 2×10^3 cells/well for 1–3 days. Then, 90 μ l of fresh serum-free medium and 10 μ l of CCK-8 reagent (Beyotime, Shanghai, China) were added to each well after decanting the old medium, and the culture was continued at 37°C for 1 h. The optical density was determined by scanning with a microplate reader (Promega) at a wavelength of 450 nm. IC₅₀ values were calculated by a DDP concentration-response curve (concentration gradient: 0, 2, 5, 10 and 20 μ g/mL for a 48-h treatment period) using GraphPad Prism 5.0 (GraphPad Software, La Jolla, CA, USA).

Flow cytometric analysis

Cells were harvested directly or 48 h after transfection and washed with ice-cold phosphate-buffered saline (PBS). The PI/RNase staining kits (Multisciences Biotech, Hangzhou, China) and annexin V-fluorescein isothiocyanate (FITC) apoptosis detection kits (Keygene Biotech, Nanjing, China) were used to detect cell cycle and apoptosis in a FACScan instrument (Becton Dickinson, Mountain View, CA), respectively.

***In situ* dUTP nick end labeling (TUNEL) assay**

Apoptosis was analyzed *in situ* using a TUNEL assay mediated by oligonucleotide-end deoxyribonucleotidyl transferase (TdT) (Beyotime) based on the manufacturer's instructions. Slides were evaluated under a light microscope. Nuclei stained with a blue dye were labeled as '−', indicating normal cells, and nuclei that were stained green were labeled as '+', indicating apoptotic cells. Cells in five fields of view were randomly counted to calculate the apoptotic rate.

***In vivo* xenograft model**

Six-week-old male BALB/c nude mice were purchased from the Laboratory Animal Center of Nanjing Medical University and maintained under pathogen-free conditions. Tumor xenografts were established by a subcutaneous injection of 0.1 mL of mock-transfected or transfected cell suspension (2×10^6 cells/mL) into nude mice on the right side of the posterior flank ($n = 5$ mice per group). Tumor growth was examined every other day. After 5–7 days, the tumor volume grew to $\approx 100 \text{ mm}^3$, and the mice were intraperitoneally injected with a suspension of PBS containing DDP (2.5 mg/kg) or PBS alone twice per week. The xenograft tumors were harvested after 4 weeks. Then, the tumor volumes were measured according to the following formula: tumor volume = length \times width² \times 0.52. The entire experimental protocol was conducted in accordance with the guidelines of the local institutional animal care and use committee.

Statistical analysis

SPSS version 16.0 (SPSS, Chicago, IL) was used for statistical analysis. The data are presented as the mean \pm standard error. Differences between groups were analyzed using Student's *t*-test for comparisons between 2 groups or one-way analysis of variance for comparisons between more than 2 groups. All tests were two-sided. $P < 0.05$ was considered statistically significant.

Disclosure statement

No potential conflict of interest was reported by the authors.

Funding

This study was supported by the National Natural Science Foundation of China [81472615].

ORCID

Sanyuan Sun  <http://orcid.org/0000-0002-7477-7491>

References

- [1] Siegel RL, Miller KD, Jemal A. Cancer Statistics, 2017. *CA Cancer J Clin.* 2017;67:7–30.
- [2] Fennell DA, Summers Y, Cadranel J, et al. Cisplatin in the modern era: the backbone of first-line chemotherapy for non-small cell lung cancer. *Cancer Treat Rev.* 2016;44:42–50.
- [3] Wen M, Xia J, Sun Y, et al. Combination of EGFR-TKIs with chemotherapy versus chemotherapy or EGFR-TKIs alone in advanced NSCLC patients with EGFR mutation. *Biologics.* 2018;12:183–190.
- [4] Shen K, Cui J, Wei Y, et al. Effectiveness and safety of PD-1/PD-L1 or CTLA4 inhibitors combined with chemotherapy as a first-line treatment for lung cancer: a meta-analysis. *J Thorac Dis.* 2018;10:6636–6652.
- [5] Ghosh S. Cisplatin: the first metal based anticancer drug. *Bioorg Chem.* 2019;88:102925.
- [6] Galluzzi L, Vitale I, Michels J, et al. Systems biology of cisplatin resistance: past, present and future. *Cell Death Dis.* 2014;5:e1257.
- [7] Fang S, Shen Y, Chen B, et al. H3K27me3 induces multidrug resistance in small cell lung cancer by affecting HOXA1 DNA methylation via regulation of the lncRNA HOTAIR. *Ann Transl Med.* 2018;6:44.
- [8] Wang X, Meng Q, Qiao W, et al. miR-181b/Notch2 overcome chemoresistance by regulating cancer stem cell-like properties in NSCLC. *Stem Cell Res Ther.* 2018;9:327.
- [9] Huang FX, Chen HJ, Zheng FX, et al. LncRNA BLACAT1 is involved in chemoresistance of non-small cell lung cancer cells by regulating autophagy. *Int J Oncol.* 2019;54:339–347.
- [10] Zhang Y, Wang X, Han L, et al. Green tea polyphenol EGCG reverse cisplatin resistance of A549/DDP cell line through candidate genes demethylation. *Biomed Pharmacother.* 2015;69:285–290.
- [11] Zhang YW, Zheng Y, Wang JZ, et al. Integrated analysis of DNA methylation and mRNA expression profiling reveals candidate genes associated with cisplatin resistance in non-small cell lung cancer. *Epigenetics.* 2014;9:896–909.
- [12] Cui Y, Gao D, Linghu E, et al. Epigenetic changes and functional study of HOXA11 in human gastric cancer. *Epigenomics.* 2015;7:201–213.

- [13] Wang L, Cui Y, Sheng J, et al. Epigenetic inactivation of HOXA11, a novel functional tumor suppressor for renal cell carcinoma, is associated with RCC TNM classification. *Oncotarget*. 2017;8:21861–21870.
- [14] Se YB, Kim SH, Kim JY, et al. Underexpression of HOXA11 is associated with treatment resistance and poor prognosis in glioblastoma. *Cancer Res Treat*. 2017;49:387–398.
- [15] Li Q, Chen C, Ren X, et al. DNA methylation profiling identifies the HOXA11 gene as an early diagnostic and prognostic molecular marker in human lung adenocarcinoma. *Oncotarget*. 2017;8:33100–33109.
- [16] Hwang JA, Lee BB, Kim Y, et al. HOXA11 hypermethylation is associated with progression of non-small cell lung cancer. *Oncotarget*. 2013;4:2317–2325.
- [17] Lu CW, Zhou DD, Xie T, et al. HOXA11 antisense long noncoding RNA (HOXA11-AS): A promising lncRNA in human cancers. *Cancer Med*. 2018;7:3792–3799.
- [18] Mu S, Ai L, Fan F, et al. Prognostic and clinicopathological significance of long noncoding RNA HOXA11-AS expression in human solid tumors: a meta-analysis. *Cancer Cell Int*. 2018;18:1.
- [19] Xue JY, Huang C, Wang W, et al. HOXA11-AS: a novel regulator in human cancer proliferation and metastasis. *Onco Targets Ther*. 2018;11:4387–4393.
- [20] Zhang Y, Chen WJ, Gan TQ, et al. Clinical significance and effect of lncRNA HOXA11-AS in NSCLC: a study based on bioinformatics, in vitro and in vivo verification. *Sci Rep*. 2017;7:5567.
- [21] Zhao X, Li X, Zhou L, et al. LncRNA HOXA11-AS drives cisplatin resistance of human LUAD cells via modulating miR-454-3p/Stat3. *Cancer Sci*. 2018;109:3068–3079.
- [22] Bhatlekar S, Fields JZ, Boman BM. HOX genes and their role in the development of human cancers. *J Mol Med (Berl)*. 2014;92:811–823.
- [23] Golpon HA, Geraci MW, Moore MD, et al. HOX genes in human lung: altered expression in primary pulmonary hypertension and emphysema. *Am J Pathol*. 2001;158:955–966.
- [24] Rauch T, Wang Z, Zhang X, et al. Homeobox gene methylation in lung cancer studied by genome-wide analysis with a microarray-based methylated CpG island recovery assay. *Proc Natl Acad Sci U S A*. 2007;104:5527–5532.
- [25] Xia B, Shan M, Wang J, et al. Homeobox A11 hypermethylation indicates unfavorable prognosis in breast cancer. *Oncotarget*. 2017;8:9794–9805.
- [26] Bai Y, Fang N, Gu T, et al. HOXA11 gene is hypermethylation and aberrant expression in gastric cancer. *Cancer Cell Int*. 2014;14:79.
- [27] Fiegl H, Windbichler G, Mueller-Holzner E, et al. HOXA11 DNA methylation—a novel prognostic biomarker in ovarian cancer. *Int J Cancer*. 2008;123:725–729.
- [28] Apostolidou S, Hadwin R, Burnell M, et al. DNA methylation analysis in liquid-based cytology for cervical cancer screening. *Int J Cancer*. 2009;125:2995–3002.
- [29] Bibikova M, Lin Z, Zhou L, et al. High-throughput DNA methylation profiling using universal bead arrays. *Genome Res*. 2006;16:383–393.
- [30] Nelson HH, Marsit CJ, Christensen BC, et al. Key epigenetic changes associated with lung cancer development: results from dense methylation array profiling. *Epigenetics*. 2012;7:559–566.
- [31] Yang X, Deng Y, He RQ, et al. Upregulation of HOXA11 during the progression of lung adenocarcinoma detected via multiple approaches. *Int J Mol Med*. 2018;42:2650–2664.
- [32] Zhang R, Zhang TT, Zhai GQ, et al. Evaluation of the HOXA11 level in patients with lung squamous cancer and insights into potential molecular pathways via bioinformatics analysis. *World J Surg Oncol*. 2018;16:109.
- [33] Matei D, Fang F, Shen C, et al. Epigenetic resensitization to platinum in ovarian cancer. *Cancer Res*. 2012;72:2197–2205.
- [34] Xu C, He T, Li Z, et al. Regulation of HOXA11-AS/miR-214-3p/EZH2 axis on the growth, migration and invasion of glioma cells. *Biomed Pharmacother*. 2017;95:1504–1513.
- [35] Qu L, Jin M, Yang L, et al. Expression of long non-coding RNA HOXA11-AS is correlated with progression of laryngeal squamous cell carcinoma. *Am J Transl Res*. 2018;10:573–580.
- [36] Liu Z, Chen Z, Fan R, et al. Over-expressed long noncoding RNA HOXA11-AS promotes cell cycle progression and metastasis in gastric cancer. *Mol Cancer*. 2017;16:82.
- [37] Zhang Y, He RQ, Dang YW, et al. Comprehensive analysis of the long noncoding RNA HOXA11-AS gene interaction regulatory network in NSCLC cells. *Cancer Cell Int*. 2016;16:89.
- [38] Chen JH, Zhou LY, Xu S, et al. Overexpression of lncRNA HOXA11-AS promotes cell epithelial-mesenchymal transition by repressing miR-200b in non-small cell lung cancer. *Cancer Cell Int*. 2017;17:64.
- [39] Latgé G, Poulet C, Bours V, et al. Natural antisense transcripts: molecular mechanisms and implications in breast cancers. *Int J Mol Sci*. 2018;19:123.
- [40] Huang B, Song JH, Cheng Y, et al. Long non-coding antisense RNA KRT7-AS is activated in gastric cancers and supports cancer cell progression by increasing KRT7 expression. *Oncogene*. 2016;35:4927–4936.
- [41] Liu C, Lin J. Long noncoding RNA ZEB1-AS1 acts as an oncogene in osteosarcoma by epigenetically activating ZEB1. *Am J Transl Res*. 2016;8:4095–4105.
- [42] Zhang CL, Zhu KP, Ma XL. Antisense lncRNA FOXC2-AS1 promotes doxorubicin resistance in osteosarcoma by increasing the expression of FOXC2. *Cancer Lett*. 2017;396:66–75.